J Electroceram (2009) 23:230–235
DOI 10.1007/s10832-007-9405-y

Structural and electrochemical properties of Nichrome anode thin films for lithium battery

Arun Patil · Vaishali Patil · Ji-Won Choi · Hyun-Jai Kim · Bong-Hee Cho · Seok-Jin Yoon

Received: 31 May 2007 / Accepted: 16 December 2007 / Published online: 6 January 2008

Abstract Low cost anode materials having a high electrochemical efficiency have been critical in the success of thin film batteries that are applicable in ubiquitous environments as a portable energy source. Nichrome thin films are ideally suited for use in hybrid assemblies but their applications include precision integrated circuits in fields of telecommunications, instrumentation, power supplies, military and medical equipment where low noise and good power dissipation are required. With such a wide spectrum of applications, it is important to understand the electric behavior of the Nichrome alloy thin films by their microstructure. In this work, nanocrystalline films of nickel chromium alloys were deposited on alumina substrate by radio frequency (RF) magnetron sputtering technology. High purity nickel and chromium sputtering target were used for the deposition. First, aluminum was deposited on ceramic substrate acts as a current collector and over that NiCr was deposited by RF sputtering method. Both the layers were analyzed for structural and electrical properties using X-ray diffraction (XRD), energy dispersive X-ray analysis (EDS), atomic force microscopy (AFM), scanning electron microscopy (SEM) and cyclic voltammetry. The XRD peak confirms that deposited NiCr and Aluminum have tetragonal and cubic structures, respectively. The crystallite size was determined by full width at half maximum of XRD peaks. Structure, composition and the properties of the film are the major focus of this paper. Composition ratio between nickel and chrome obtained by EDS is 1:1. Particle size and microstructure of the film have been studied by SEM and AFM. Electrochemical properties of the films were analyzed. Reaction mechanism for the insertion and excretion is reported. After Lithium insertion and extraction the effect on the surface and structure of the thin film has been studied. The composition of equilibrium phases of NiCr as useful as attracting anode for the thin film battery. Nichrome on aluminum thin films as an anode has been attracted because it provides practical advantages including low cost production and competitive electrical performance.

Keywords Ni-Cr alloy · Thin film · Anode · Secondary lithium batteries

A. Patil · V. Patil · J.-W. Choi · H.-J. Kim · S.-J. Yoon (✉)
Thin Film Materials Research Center,
Korea Institute of Science and Technology,
Seoul 136-791, Republic of Korea
e-mail: sjyoon@kist.re.kr

B.-H. Cho
Department of Electrical Engineering,
The University of Suwon,
Hwaseong 445-743, Republic of Korea

1 Introduction

Nanostructured materials are becoming increasingly important for electrochemical energy storage [1–5]. New materials hold the key to fundamental advances in energy conversion and storage. Nanomaterials offer unique properties or combinations of properties as electrodes and electrolytes in a range of energy devices. Recent studies of lithium ion batteries focus on improving electrochemical performance of electrode materials and lowering cost. Considerable improved electrochemical performance of the electrode materials has been achieved. There are still problems needing further investigation including theoretical aspects, which will in the meanwhile stimulate the investigation for better electrode materials. Throughout the search for carbon alternatives, much effort has been devoted to the use of metal alloys.

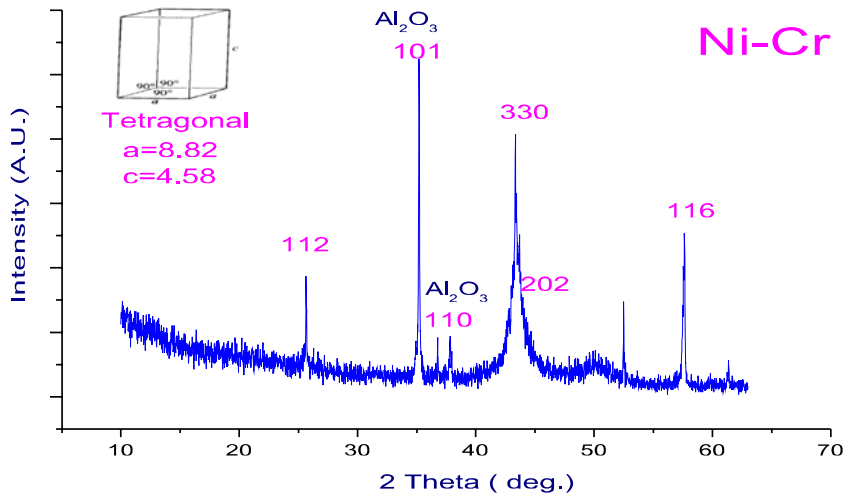

Fig. 1 X-ray diffraction pattern for Ni-Cr thin film

We present nanocrystalline films of nickel chrome alloy deposited on ceramic substrates as anode for the development of lithium based rechargeable batteries. Low cost anode materials having a high electrochemical efficiency have been critical in the success of thin film batteries that are applicable in ubiquitous environments as a portable energy source. Which has also many advantages include (1) better accommodation of the strain of lithium insertion/ removal, improving cycle life; (2) new reactions not possible with bulk materials; (3) higher electrode/electrolyte contact area leading to higher charge/discharge rates; (4) short path lengths for electronic transport and (5) short path lengths for Li+ transport [6–7].

Lithium metal has commonly been used as anodes for rechargeable thin-film micro batteries which can be employed as power sources for micro devices. However, lithium metal has some problems for the application due to its low melting point, high reactivity with air, and tendency to form dendrites. Hence, there is currently a significant interest in finding new anode materials [8–10]. Alloy-based materials containing such lithium storage metals as Al, Si and Sn have been extensively studied as anodes for lithium-ion batteries. However, these alloy systems undergo large volume changes during Li insertion/ extraction cycling [11–13]. This limits the mechanical stability and cycle life of the electrode. Recently, intermetallic compounds or alloys AM have been widely studied, where A is an "active" alloying element and M is an "inactive" element [14, 15]. The performance of alloy electrodes can be improved significantly when the active alloying elements are finely dispersed with an inactive component in a composite matrix. In addition, intermetallic alloys, show improved electrochemical cycling performance compared to pure [16].

Nichrome thin films have a wide spectrum of applications, it is important to understand the electric behavior of the Nichrome alloy thin films by their microstructure. There is a great body of literature dealing with bulk solid-state phase transformations in different materials but considerably less information is available on the same subject in thin films, specifically where the thin film is deposited from a source having composition in the two- phase region of a phase diagram. In this work, we have made an effort to study the microstructure of the deposited thin films of NiCr alloy compositions on aluminum current collector. The sample is analyzed for structural and morphological using X-ray diffraction (XRD), scanning electron microscopy (SEM) and atomic force microscopy (AFM) techniques.

In this investigation, we report, first time, the preparation, structural and electrochemical performance of nanocrystalline intermetallic NiCr alloy anode with aluminum current collector.

2 Experimental details

Nickel-chromium alloy thin films of compositions 50:50 ratios in wt.% were deposited on aluminum current collector. Aluminum current collector was deposited on

Table 1 EDS result shows pure Ni-Cr deposited on aluminum substrate film.

Element	Weight%	Atomic%
Al	39.64	57.38
Ni	29.66	21.53
Cr	30.70	21.09
Total	100	

Table 2 EDS result shows pure Al deposited on Al_2O_2 substrate film.

Element	Weight%	Atomic%
O	44.45	57.44
al	55.55	42.56
Totals	100.00	

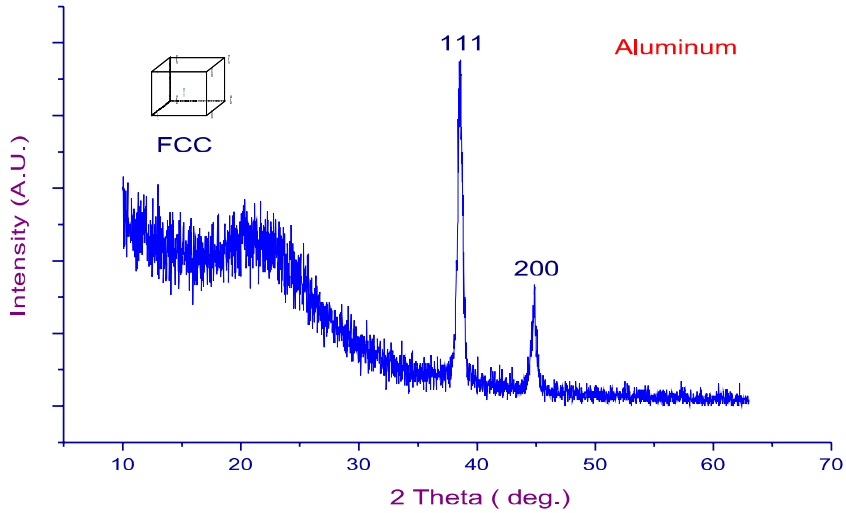

Fig. 2 X-ray diffraction pattern of Aluminum thin film

ceramic substrates by radio frequency (RF) sputter deposition technique. The target composition of deposited Nichrome and aluminum films were characterized by energy dispersive X-ray analysis (EDS) to ensure identical composition of the target and the films. The surface microstructure was determined by SEM and AFM. The XRD experiments were carried out with CuKα radiation. Cyclic voltammetry (CV) properties was measured with the cell which was composed of a metal Lithium foil as a counter electrode 1MLiPF$_6$ in 1:1 (*v*/*v*) mixture of ethylene carbonate (EC) and diethyl carbonate (DEC) as Electrolyte. Cells were fabricated to test the electrochemical properties of thin-film electrodes. The cells were assembled in an argon filled glove-box. AFM and SEM images of 50:50 wt.% NiCr and aluminum films were taken before and after cycling. Film thickness was measured by cross sectional SEM and from XRD.

3 Results and discussion

An X-ray diffraction pattern of NiCr alloy thin film is shown in Fig. 1. The experimental XRD data is in good agreement with the Joint Committee on Powder Diffraction Standards (JCPDS) data. The XRD data of the as deposited 50:50 wt.% NiCr composition shows two clear main peak at 43.25 and 44.43 with hkl plane 330 and 202 respectively and indicates that deposited NiCr is in tetragonal structure (JCPDF card no. 26-0430). From the width of the diffraction peaks, the average grain size was calculated according to the Scherrer equation (crystallite size $D = 0.9\lambda/B\text{Cos}\theta$)] using traces program (Traces Program, Diffraction Technology, Australia) where λ is the X-ray wavelength, B the angular line width at the half maximum intensity and θ the Braggs angle. The estimated average crystallite size for the NiCr alloy deposited on thin film is about 25 nm. Composition ratio between nickel chrome and for pure aluminum was obtained by EDS as shown in Tables 1 and 2. Table 1 show that the deposited NiCr is in 1:1 ratio. Table 2 shows EDS of pure aluminum deposited on the ceramic substrate. The X-ray diffraction pattern of aluminum current collector deposited in thin film form on the ceramic substrate is shown in Fig 2. The experimental XRD data is in good agreement with the standard JCPDS data (JCPDF card no. 26-0430). The XRD data of the as deposited pure aluminum shows two clear main peaks at 38.474 and 44.72 with hkl plane 111 and 200 respectively and indicates that deposited aluminum is in face centered cubic structure (JCPDF card no. 85-1327). The average grain size was 35 nm calculated according to the Scherrer equation [17]. Some amorphous nature is observed in X-ray diffraction which is confirmed from the SEM image Fig. 3a. Figure 3b shows the cross sectional SEM image of the aluminum current collector from which thickness calculated was about 8.2 µm. Figure 3c is the AFM image of the aluminum thin film. Root mean square roughness Rq is 11.2 nm and indicates that the deposited film is very smooth.

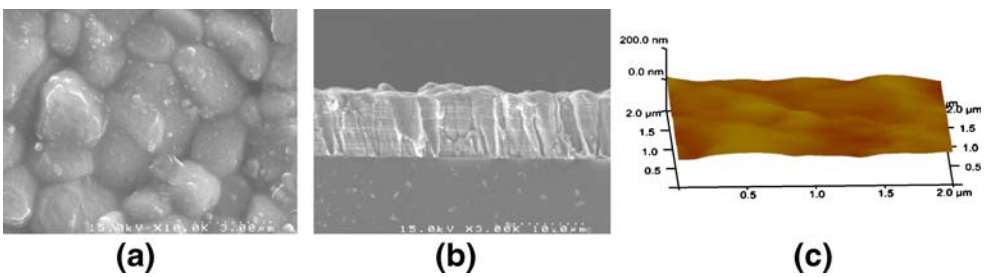

Fig. 3 **a** SEM image of Aluminum on ceramic substrate **b** cross sectional SEM image of Ni-Cr thin film **c** AFM of Aluminum thin film

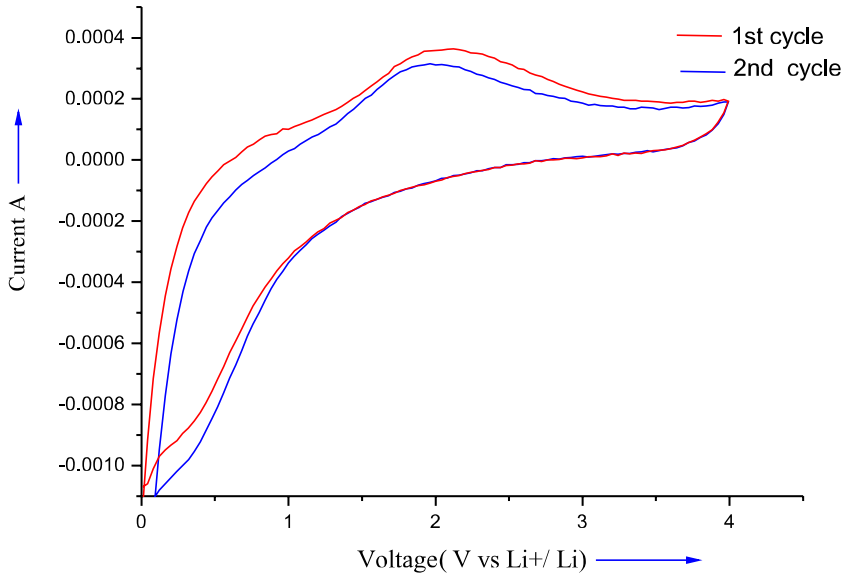

Fig. 4 The cyclic voltammogram of Ni-Cr thin film

In the NiCr electrode, the element Cr is inactive to Li and only Ni can react with Li to form a series of LiNi*x* alloys. Thus, the following mechanism was proposed for the reaction of NiCr with Li in lithium cells, [18]

$$xLi^{+} + xe^{-} + CrNi \rightarrow LixNi + Cr \quad \text{insertion}$$

$$xLiNi + Cr \rightarrow CrNi + xLi^{+} + xe^{-} \quad \text{de insertion}$$

In the electrochemically formed LiNi alloys, lithium is stored in the ionic state and not in atomic form. Thus, Ni accepts electrons to become Ni^{-} [19]. After the first discharge, when lithium was extracted from the alloy electrode, it is supposed that Ni and Cr are kept in their elementary states. In that case, Cr will act as buffering matrix for the formation of LiNi in the subsequent cycle. This would help to prevent cracking of the alloy particles, which is essential for good cyclability of the NiCr electrode. It was indicated that the structure that allows Li and Ni, Cr and Ni to reversibly alloy/dealloy is the key to gain high capacity long-life anode materials. NiCr has been able to realize such reversible reactions, hence resulting in the high cycle performance.

The film thickness and crystal particle size varied largely upon cycling, and formation of cracks and pores were seen with cycling. With the first charging discharging process, the dense film became porous. Decrease in the crystal size of the film was also confirmed with cycling. This may be due to the reaction where Li transforms into the NiCr phase to generate Ni-rich and Li–Ni alloy phases, and to the converse reaction where Li goes out from the Li–Ni alloy and Ni rich phases to generate NiCr phases. This reversible reaction could be contributing to the good anode property of nickel and chromium

Figure 4 shows the CV performance of NiCr film anode. CV properties was measured with the cell which was composed of a metal lithium foil as a counter electrode and 1M $LiPF_6$ in 1:1 (*v*/*v*) mixture of EC and DEC as electrolyte. Cells were fabricated to test the electrochemical properties of thin-film electrodes. The cells were assembled in an argon filled glove-box.

The electrochemical tests have been started with slow voltammetric measurements of Ni-Cr anode thin film. The first cycle shows two lithiation peak at about 0.1 and 0.4 V and the delithiation peak is at about 0.2 V. The voltage values of the first lithiation and delithiation peaks are typical for this active material. The voltage values of the lithiation peaks of the second cycle are 0.09 and 0.38 V. The delithiation value is 0.17 V in second cycle.

The voltage value of the second lithiation and delithiation peak drops, comparing to that from the first cycle. This

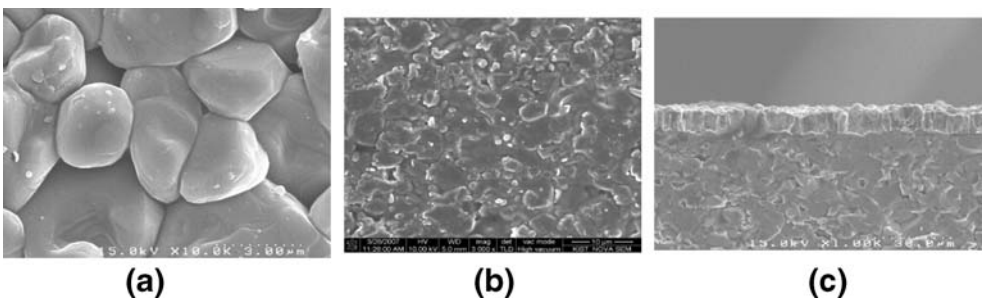

Fig. 5 **a** SEM image of Ni-Cr before cycling **b** SEM image of Ni-Cr after cycling **c** cross sectional SEM image of Ni-Cr thin film

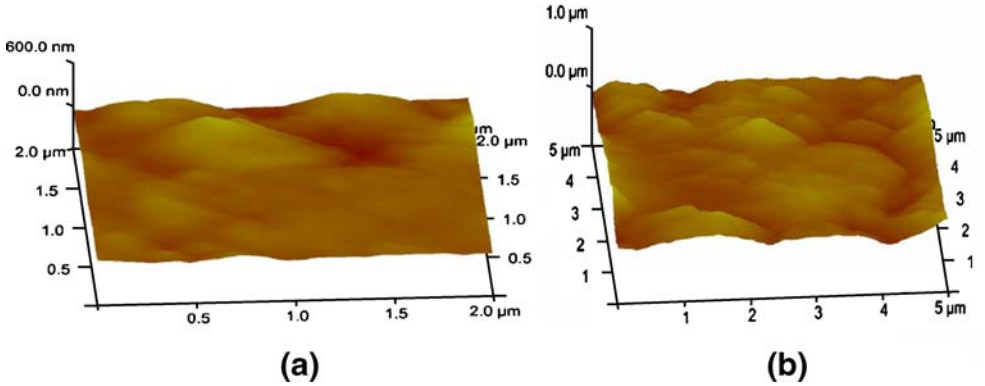

Fig. 6 **a** AFM image of Ni-Cr before cycling **b** AFM image of Ni-Cr after cycling

polarization drop most probably is due to the re-ordering of the structure after first lithiation. NiCr film exhibits superior electrochemical performance [20]. The difference of polarization drop of Ni-Cr film anode in EC and DEC as electrolyte may be attributed to the different properties of solid electrolyte interphase (SEI) layer formed in initial cycle.

SEM images of NiCr film anodes before and after cycling are shown in Fig. 5. Both these alloy compositions lie in the two-phase region of the nickel-chromium binary phase diagram due to the limited solubility of nickel in chromium [1]. Figure 5c shows the cross sectional SEM of NiCr thin film. Thickness is about 4.1 µm. Figure 5a shows that quite homogeneous NiCr alloy film prepared by RF sputtering. Due to the ultra fine nature of the NiCr alloy particles; these small particles tend to form large agglomerates. The surface of NiCr film is clean and smooth before cycling. When the NiCr film electrode is charged to 0.8 V, the surface is covered with the SEI layer which is the reduction product of electrolyte including solvent and salt anion. The SEI layer formed in electrolyte is non homogeneous and embeds with some spherical particles with about 100–200 nm in size, as shown in Fig. 5b.

However, the SEI layer displays a series of cracks in the valleys between the hills. We think that the cracks are caused by the shrinkage of NiCr film during lithium ions extraction. When the lithium ions are extracted from NiCr electrode, most of the contraction of Cr layer must be in the vertical direction to the substrate. SEI layer in the valleys cannot bear the contraction stress of the two sides of walls of the valley, resulting in the cracks. It is concluded that the presence of $LiPF_6$ in electrolyte results in very different surface morphology of the SEI layer and configuration of LiF, which may be the key factors to the electrochemical performance of NiCr film.

The electrolyte can form the SEI layer during cycling. Therefore, a new SEI layer is formed constantly on the surface of NiCr film in each cycle, resulting in the increasing of thickness of SEI layer. This then causes the increasing of anode polarization, which degrades the electrochemical performance of NiCr film.

This suggests that with repeated cycling, some Li gets trapped within the Li–Ni alloy, unable to dealloy during the discharge process. The SEM images show the similar cracked surface morphology as Fig. 5b. Thickness of the as-deposited NiCr was calculated from the cross sectional SEM. The observed thickness was about 4.1 µm (Fig. 5c). The change of the electrode crystallinity with cycling was also evaluated. Li insertion has a significant effect on lowering the crystallinity of the electrode structure in the nanometer scale. Figure 6 shows the AFM image of the NiCr before and after cycling. Mean surface roughness (Rq) before and after cycling was 23 and 73 nm respectively. With the Li+ insertion during the charge process, Ni atoms segregate from the NiCr alloy structure and alloys with Li to form the Li–Ni alloy phase. This reaction should be reversible. With discharge, the Li^+ is extracted from the Li–Ni alloy phase, and the dealloyed Ni atom gets absorbed into the Cr matrix again forming the CrNi alloy phase.

Considering this reaction mechanism on the cycle performance and structural changes of the electrodes, it may be suggested that the structure of Ni_{50}–Cr_{50} was unable to free the Ni from the metastable alloy crystal to allow its full alloying with Li. This could also be supported by the fact that the initial cycle shows lithiation peak at about 0.1 and 0.4 V and the delithiation peaks is at about 0.2V and for second cycle lithiation at 0.09 and 0.38 V and delithiation at 0.17 V, respectively [21].

4 Conclusions

XRD studies showed that the deposited NiCr and aluminum are in tetrahedral and cubic structures, respectively. During lithium insertion into the alloy electrode Ni acts as an active center which reacts with Li to form Li*x*Ni alloys. The reaction is reversible. Addition of lithium results in ductile alloys which greatly reduces the volume change. Nickel enters interstitially into Cr Lattice providing space for Li. Nickel can promote the diffusion of lithium in the of alloy materials and effectively prevents

the production of dendrites. SEM suggests that with repeated cycling, some Li gets trapped within the Li–Ni alloy, unable to dealloy during the discharge process. Li insertion has a significant effect on lowering the crystallinity of the electrode structure in the nanometer scale. Optimizing the composition of NiCr could lead to the improvement of the electrochemical performance of this electrode material. We expect the composition of equilibrium phases of NiCr will be useful for the attracting anode for the thin film battery.

Acknowledgements One of the author Dr. Arun Patil would like to thank to Hon. Rajkumar Agarwal Chairman of the Bansilal Ramnath Agarwal Charitable Trust, Pune, India, Mr. Bharat Agarwal and Prof. S. B. Mantri for deputing to the Korean Institute of Science and Technology, Seoul, South Korea.

References

1. L.F. Nazar et al., Int. J. Inorg. Mater. **3**, 191 (2001)
2. M. Hirshes, Mater. Sci. Eng. B **108**, 1 (2004)
3. S. Santhanagopalan, J. Power Sources **156**(2), 620 (2006)
4. T. Moon, C. Kim, B. Park, J. Power Sources **155**(2), 391 (2006)
5. J. Schwenzel, V. Thangadurai, W. Weppner, J. Power Sources **154** (1), 232 (2006)
6. M. Winter, J.O. Besenhard, M.E. Spahr, P. Novak, Adv. Mater. **10**, 725 (1998)
7. A.S. Arico, P. Bruce, B. Scrosati, J.-M. Tarascon, W. Van Schalkwijk, Nature **4**, 366 (2005)
8. I.C. Kim, D.B.J. K. Lee. J. Electroceram. **17**, 661 (2006)
9. C.M. Kleinlogel, L.J. Gauckler, J. Electroceram. **5**, 231 (2000)
10. J.H. Joo, G.M. Choi, J. Electroceram. **17**, 1019 (2006)
11. M. Winter, J.O. Besenhard, Electrochim. Acta **45**, 31 (1999)
12. O. Mao, R.A. Dunlap, I.A. Courtney, J.R. Dahn, J. Electrochem. Soc. **145**, 4195 (1998)
13. K.D. Kepler, J.T. Vaughey, M.M. Thackeray, Electrochem. Solid-State Lett. **2**, 307 (1999)
14. O. Mao, J.R. Dahn, J. Electrochem. Soc. **146**, 414 (1999)
15. A.R. Miedema, Philips Tech. Rev. **36**, 217 (1976)
16. J.B. Bates, N.J. Dudney, B. Neudecker, A. Ueda, C.D. Evans, Solid State Ion. **135**, 33 (2000)
17. A.R. Patil, V.N. Patil, P.N. Bhosalea, L.P. Deshmukh, J. Mat. Chem. Phy. **65**, 266 (2000)
18. M. Winter, J.O. Besenhard, J.H. Albering, J. Yang, M. Wachtler, Prog. Batteries Battery Mater. **17**, 208 (1998)
19. M. Winter, J.O. Besenhard, Electrochim. Acta **45**, 31 (1999)
20. P. Zuo, G. Yin, J. Alloy Comp. **414**, 265 (2006)
21. H. Mkaibo, T. Momma, T. Osaka, J. Power Sources **146**, 457 (2005)